

Cyclic voltammetry studies of Cd^{2+} and Zn^{2+} complexation with hydroxyl-terminated polyamidoamine generation 2 dendrimer at a mercury microelectrode

Alexander B. Nepomnyashchii, Mario A. Alpuche-Aviles, Shanlin Pan, Dongping Zhan, Fu-Ren F. Fan, Allen J. Bard*

Department of Chemistry and Biochemistry and Center for Electrochemistry, The University of Texas at Austin, 1 University Station A5300, Austin, TX 78712-0165, United States

Received 26 November 2007; received in revised form 28 January 2008; accepted 30 January 2008
Available online 8 February 2008

This paper is dedicated to Israel Rubinstein on his 60th birthday.

Abstract

Cyclic voltammetry was used to determine the stability constants for the complexation of cadmium and zinc ions with hydroxyl-terminated polyamidoamine generation 2 dendrimers with an ethylenediamine core (PAMAM G2-OH) at a mercury ultramicroelectrode. Cadmium and zinc ions were found to form poly-metal complexes through the interactions with interior amino groups rather than hydroxyl groups and the maximum number of metal ions per dendrimer or stoichiometry was 4. Complexation is accompanied by a significant decrease in the limiting current and by measuring the changes in the magnitude of cathodic current with the analytical dendrimer:metal ion ratio and fitting the resulting curves, the four cumulative consecutive complexation constants were determined: $1.3 \times 10^5 \text{ M}^{-1}$, $1.6 \times 10^9 \text{ M}^{-2}$, $3.3 \times 10^{12} \text{ M}^{-3}$ and $4.6 \times 10^{14} \text{ M}^{-4}$ for Cd^{2+} and $1.0 \times 10^6 \text{ M}^{-1}$, $1.6 \times 10^9 \text{ M}^{-2}$, $4.6 \times 10^{14} \text{ M}^{-3}$ and $2.6 \times 10^{17} \text{ M}^{-4}$ for Zn^{2+} . The stronger interaction of zinc ions with PAMAM G2-OH compared to cadmium was accompanied with a sharper decrease of the cathodic current with the addition of dendrimer and a larger half-wave potential shift than cadmium. This was rationalized by evaluating the changes of the diffusion coefficients for these two different systems by electrochemical means.
© 2008 Elsevier B.V. All rights reserved.

Keywords: Cyclic voltammetry; Mercury microelectrode; Complexation constant; Dendrimer

1. Introduction

Dendrimers are highly ordered branched macromolecules with repeating fragments. PAMAM dendrimers were first synthesized two decades ago by Tomalia et al. [1,2] and have since become well-characterized and widely studied systems. The highly branched dendritic structure has advantages over other macromolecular systems and can be potentially used for drug delivery [3], catalysis [4,5], and, extraction of aqueous waste [6–9] under optimal conditions. Recent studies have shown that PAMAM dendri-

mers can interact with metal ions through their interior or exterior complexing groups, and can serve as precursors in the preparation of metal nanoparticles. For example, Pt [4], PtPd [5] and Au [10] nanoparticles have been synthesized with PAMAM. However, the thermodynamics and detailed mechanism of the complexation process of dendrimers with metals and metal ions is still not clear.

Absorption spectroscopy, filtration, polarography, potentiometry and other electrochemical methods can be used to study the complexation process of dendrimers with metals [11,12]. Cyclic voltammetry (CV) is especially useful in probing the nature of the metal–dendrimer complexation process. For example, CV has been used to characterize the interaction of silver ions with dendrimers at an inlaid

* Corresponding author. Tel.: +1 512 471 3761; fax: +1 512 471 0088.
E-mail address: ajbard@mail.utexas.edu (A.J. Bard).

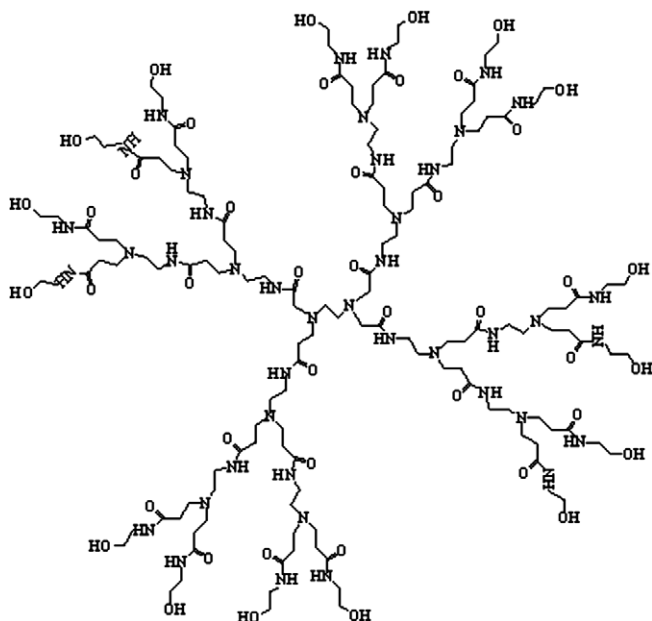


Fig. 1. Chemical structure of PAMAM G2-OH dendrimer.

macro gold or platinum disk electrode [13] and to study redox labeled dendrimer systems [14,15]. One of the disadvantages of studying metal-ion complexation by CV is the frequent occurrence of non-nernstian behavior of metal ions at a solid metal electrode surface [16,17]. Mercury has a defect-free and renewable surface and reversible electrochemical behavior is frequently found for metal ions when amalgam formation occurs. For example, it has been widely used in polarography to measure the stability constants (K_L , where L is the number of ligands per central metal) [17].

In this report, we used a mercury ultramicroelectrode (UME) to study the complexation characteristics of zinc and cadmium ions with generation 2 PAMAM (G2-OH) dendrimer (Fig. 1). The UME is also useful in measuring both steady-state limiting currents and, with fast scan rates, in studying short-lived intermediates [18,19]. Cadmium and zinc have long been known to show good behavior at the mercury electrode [20] and stable and reproducible cyclic voltammograms were obtained with G2-OH. Our results indicate that cadmium and zinc can form poly-metal complexes through the interactions with interior amino groups and the maximum coordination number of metal ions per PAMAM G2-OH is 4. The stability constants K_q (where $q = 1-4$, represents the number of metal ions per dendrimer) were determined by fitting the experimental results, and a stronger interaction of Zn^{2+} compared to Cd^{2+} with PAMAM G2-OH was observed.

2. Experimental section

2.1. Chemicals

Generation 2 hydroxyl-terminated PAMAM dendrimer with an ethylenediamine core, $Hg_2(NO_3)_2$, $Zn(NO_3)_2$,

$Cd(NO_3)_2$, citric acid, Na_2HPO_4 were purchased from Aldrich Chemical Co. (Milwaukee, WI); KNO_3 , $NaNO_3$ and agar was from Fisher Sci. Co. (Fair Lawn, NJ); hexamineruthenium (III) chloride was obtained from Strem Chemicals (Newbury Port, MA). All the compounds were used without further purification. High-purity water (resistivity $\rho = 18 M\Omega cm$) (Milli-Q, Millipore Corp., Billerica, MA) was used in all experiments, and all solutions were deaerated with argon for 30 min.

2.2. Apparatus and methods

The mercury UME was prepared by following the procedure of Wehmeyer and Wightman [18]. Briefly, a $10 \mu m$ diameter Pt disk microelectrode was polished with $0.3 \mu m$ alumina (Buehler, Lake Bluff, IL) and further sonicated in 95% solution of ethanol. A solution of 5.7 mM mercurous ion was used for Hg deposition and 0.5% concentrated nitric acid in 1 M KNO_3 was added to prevent hydrolysis of the mercurous ions. Mercury was deposited on the Pt UME, recording the current transient at a potential of 0.1 V vs SCE for 333 s. Fig. 2 shows a schematic drawing of the mercury UME formed in this manner. The radius of the mercury UME produced was determined as $7 \mu m$ from steady-state voltammograms of cadmium nitrate solutions at several concentrations. The mercury could be stripped off of the platinum surface by applying a positive potential of 0.5 V (vs SCE) at the end of the experiment to avoid contamination of the Pt electrode. A fresh Hg UME was prepared for every set of experiments. A three compartment electrochemical cell, with working electrode, platinum wire auxiliary electrode and SCE reference electrode, was used for electrochemical experiments involving titration of metal ion with dendrimer. A 2% solution of the agar gel in 0.2 M $NaNO_3$ aqueous solution was used as a salt bridge to the SCE to avoid any possible contamination of the test solution by chloride and mercury ions. PAMAM G2-OH ($M_w = 3272 g/mol$) was used as the titrant for both Cd^{2+} and Zn^{2+} . As PAMAM G2-OH is added to the metal ion solution, the viscosity increases and this affects the measured limiting current. A viscosity correction was made using $0.6 mM Ru(NH_3)_6^{3+}$ at pH 3 in a buffer composed of 0.2 M Na_2HPO_4 and 0.1 M citric acid. All solutions were purged with argon for 30 min prior to every

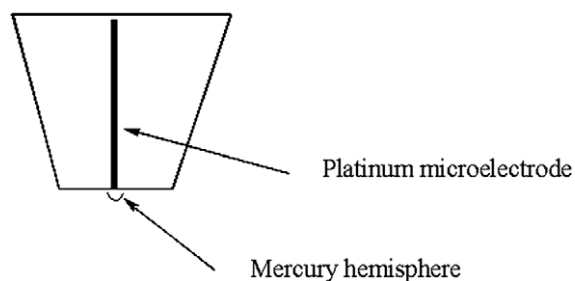


Fig. 2. Schematic drawing of a mercury hemispherical electrode fabricated on a platinum microelectrode by electrochemical deposition.

electrochemical measurement. A CHI 660 electrochemical station (CH Instruments, Austin, TX) was used for all electrochemistry measurements.

3. Results

3.1. Reduction of Cd^{2+} in the absence of dendrimers at the hemispherical mercury UME

The electrochemical behavior of metal ions at a mercury UME are different from those at a bare platinum or large hanging mercury electrode. The steady-state current of metal ions at a hemispherical Hg UME can be expressed as

$$i_{\text{ss}} = 2\pi nFDcr, \quad (1)$$

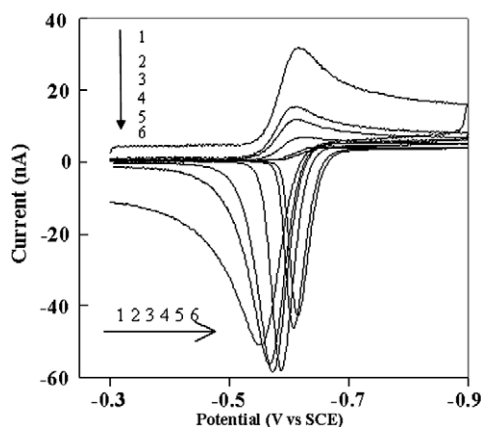


Fig. 3. Cyclic voltammograms of 0.6 mM $\text{Cd}(\text{NO}_3)_2$ at a mercury microelectrode at different scan rates; (1) 50 V/s; (2) 10 V/s; (3) 5 V/s; (4) 1 V/s; (5) 0.1 V/s; (6) 0.05 V/s. The vertical arrow points to decreasing scan rate for decreasing cathodic current while the horizontal arrow points to decreasing scan rate for increasing negative potential shift of the anodic stripping peak. Supporting electrolyte: 0.2 M NaNO_3 . Electrode radius: 7 μm .

where n is the number of the electrons transferred, r is the radius of a hemispherical electrode and D is the diffusion coefficient of the metal ion. Since the UME was made by electrodeposition in our experiment, the radius of the electrode can be estimated from the deposition time, t , assuming a diffusion-controlled deposition of a mass of Hg and a volume of mercury $V = 4/3\pi r^3$

$$r = [2MD_{\text{M}}Ct/\rho]^{1/2}, \quad (2)$$

where M is the molecular weight and ρ is the density of Hg, and D_{M} is the diffusion coefficient of mercurous ions. [18] Cyclic voltammograms of cadmium ions at a Hg UME, at scan rates, v , of 0.05–50 V/s (Fig. 3) showed a slight shift of the half-wave potential to more negative values with a decrease of v . Such scan rate dependence at a Hg UME is similar to that seen with mercury thin film electrodes and is caused by saturation of the amalgam with metal at slow scan rates [21–23]. The experimental results for the reduction of Cd^{2+} at the Hg UME were very close to digital simulation results (Fig. 4). Digital simulations were established by using Digielch 2.0 software [24]. The disparity between the experimental and the simulated oxidation current may partially be due to the modeling problem of simulation and partially due to the incomplete stripping of the cadmium from the mercury. The latter suggests that a large quiet time must be used to regenerate a clean mercury drop. In the simulation, a spherical electrode was assumed and then corrected by a factor of 1/2 for a hemisphere to obtain the results shown by Fig. 5a. This assumption might not be completely appropriate to simulate the diffusion current within an electrode with spherical-segment geometry, e.g. a hemisphere. Simulations were established assuming very fast heterogeneous kinetics ($k^0 = 10^5 \text{ cm/s}$) and the measured uncompensated resistance and capacitance values of 21 k Ω and 1×10^{-10} F, respectively. Diffusion coefficients were found

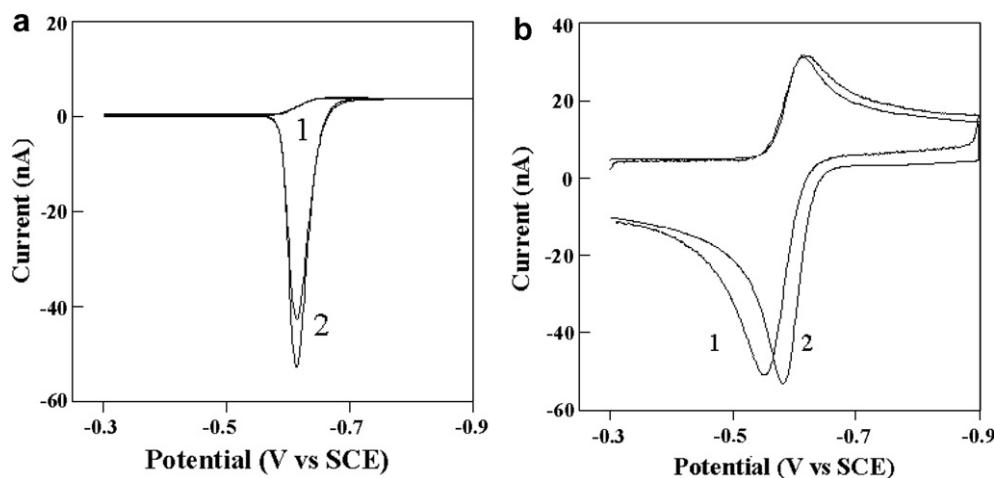


Fig. 4. Experimental (1) and simulated (2) cyclic voltammograms of 0.6 mM $\text{Cd}(\text{NO}_3)_2$. Scan rate: (a) 50 mV/s; (b) 50 V/s. Experimental data: supporting electrolyte: 0.2 M NaNO_3 . Electrode radius 7 μm . Simulated data: diffusion coefficient of Cd^{2+} was $6.8 \times 10^{-6} \text{ cm}^2/\text{s}$ and for the metal stripping $8.0 \times 10^{-6} \text{ cm}^2/\text{s}$; Uncompensated resistance: 21 k Ω ; capacitance: 1×10^{-10} F.

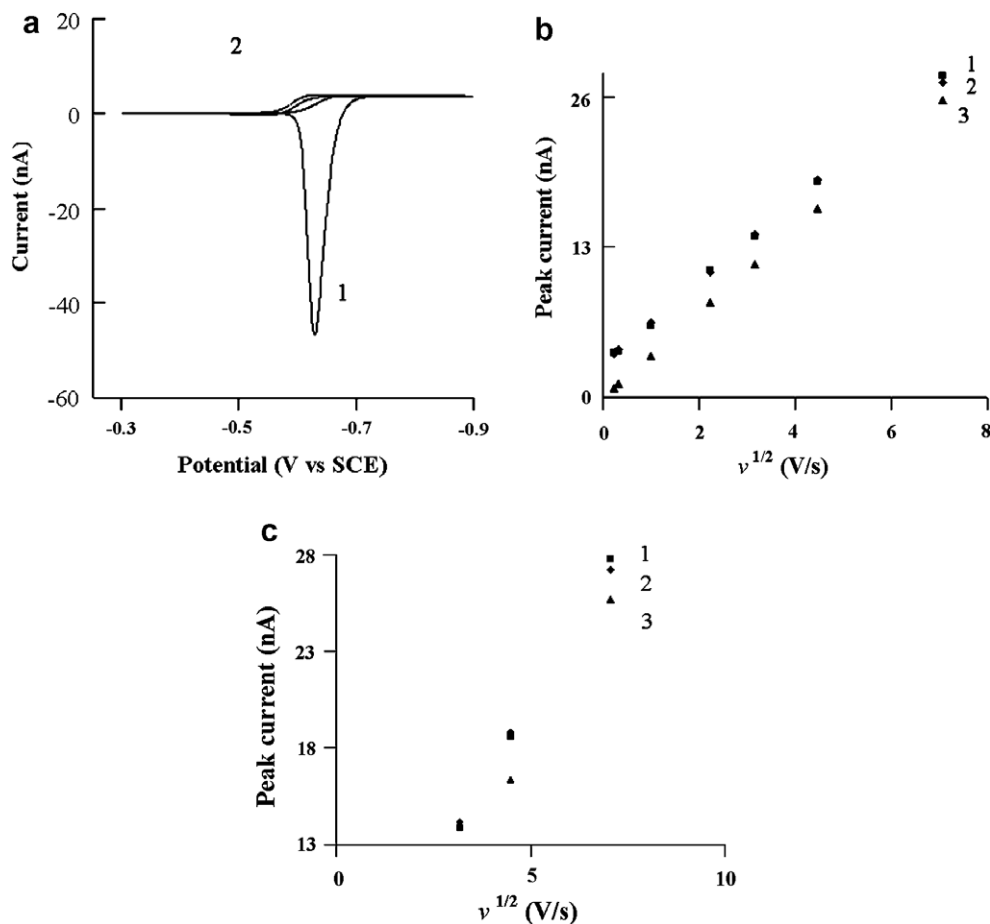


Fig. 5. (a) Experimental cyclic voltammogram (1) of 0.6 mM metal ions under radial diffusion control at a hemispherical mercury electrode and simulated data (2) under radial diffusion control without film formation; scan rate 50 mV/s. (b) Scan rate dependence of the peak current of the cyclic voltammograms for metal ions under radial diffusion control (1: simulated; 2: experimental data) in comparison of the one under planar diffusion control (3: simulated results); (c) expanded plot of the *b* in the peak current range from 13 to 28 nA. For the experimental data: supporting electrolyte: 0.2 M NaNO₃. Electrode radius 7 μm. Simulated data: Diffusion coefficient of Cd²⁺ was 6.8×10^{-6} cm²/s and for the metal stripping 8.0×10^{-6} cm²/s; Uncompensated resistance: 21 kΩ; capacitance: 1×10^{-10} F.

to be 6.8×10^{-6} cm²/s for the reduction of cadmium ions and 8.0×10^{-6} cm²/s for the stripping of cadmium metal from mercury. Usually the stability constants *K* of the coordination reactions between metal ions and organic species are determined by measuring the potential difference in the voltammetry of free metals to the ligand-bound ones [20]. However, cadmium shows a negative potential shift at low scan rate at a Hg UME, limiting the use of a slow scan rate to determine the stability constants through potential shifts (Figs. 3 and 5a). Therefore fast scan rates of 1 V/s or higher were used to determine the complexation parameters of cadmium based on the potential shift after a complex formed with other ligands. In this case the formed amalgam is not saturated and thus the experimental conditions are close to those for a simple diffusion-controlled process of metal ions in solution. Fast scans can be used for current measurements, where the electrochemical reduction of the metal ions at the Hg UME can be treated by planar-diffusion and the Randles–Sevcik equation used for current calculations. The

region between the spherical and planar diffusion-controlled processes is less convenient to treat. Since the amalgam film is not saturated with Cd, metal diffusion inside the mercury film leads to electrochemical behavior characteristic of diffusion control with no potential shift as a function of *v*. The slow scan rate experiments show that the steady-state current is the same at Hg UME as that of a regular hemispherical electrode without influence of amalgam formation (Fig. 5a). This combination of slow and fast scan rate CV allows us to determine the character of the binding between dendrimer macromolecule and metal ions. The experimental and theoretical scan rate dependences of cathodic peak current are presented in Fig. 5b. There is a change from hemispherical to planar diffusion with an increase in scan rate. At 30 and 50 V/s the square root scan rate dependence is close to linear, indicating diffusion control. The line does not extrapolate to zero due to the small contribution of the radial diffusion as evident from the simulation of hemispherical UME (Fig. 5a).

3.2. Reduction of the Zn^{2+} in the absence of dendrimers at hemispherical Hg UME

Similar to electrochemical behavior of Cd^{2+} at the Hg UME, zinc also forms amalgams at the mercury electrode surface after reduction (Fig. 6). The reduction peak current shows a behavior close to a linear square root scan rate dependence, suggesting diffusion control at the Hg UME. The oxidation peak broadening in the CVs is due to the heterogeneous kinetic limitations of the electrode reaction.

3.3. Complexation studies of the PAMAM G2-OH dendrimers with Cd^{2+} and Zn^{2+} ions

Addition of the bulky ligand to the metal ions has two effects: a significant decrease in the diffusion coefficient and a negative shift in the potential of the wave. The CVs of Cd^{2+} in the presence of G2-OH at scan rates of 50 V/s and 50 mV/s in Fig. 7 show the pronounced negative shift in the reduction potential. A similar shift in the reduction peak upon addition of dendrimer was observed for silver–dendrimer G2-OH complex [13]. Compared with Zn^{2+} , as we will discuss below in more detail, the reduction peak potential shift for Cd^{2+} is relatively small because of weaker interaction between Cd^{2+} and the dendrimer. The shift of the oxidation reaction to more positive potential with v is ascribed to the effect of slower heterogeneous kinetics.

One can study the complexation by titrating a solution of the metal ion with dendrimer and noting the ratio of total metal ions to total ligand. A decrease in the reduction current was obtained for Cd^{2+} when PAMAM G2-OH was added to the electrolyte to form complexes. The decrease in reduction current is due to a decrease of the amount of free Cd^{2+} and the formation of metal–dendrimer complexes, which have smaller diffusion coefficients than free Cd^{2+}

ions. The cyclic voltammograms for the free Cd^{2+} and the largely complexed Cd^{2+} and their scan rate dependence are shown in Fig. 7. A linear dependence of cathodic current on $v^{1/2}$ at $v > 1$ V/s shows a diffusion-controlled process for the formed metal–dendrimer complex (Fig. 7d). The metal–dendrimer binding stability and other characteristics can be studied by measuring the dependence of the reduction current on $R = C_D/C_M$, where C_D and C_M are the analytical concentrations of dendrimer and metal, respectively. As shown in Fig. 8, a dramatic decrease of the steady-state current after the initial addition of the dendrimer, with a very slow decrease in the presence of the excess dendrimer is seen in the titration results. The former decay is due to the metal–dendrimer complex formation and the later is caused by the changes of solution viscosity induced by the excess amount of dendrimer. The magnitude of current decay caused by the viscosity increase can be estimated by addition of the same amount of dendrimer to 0.6 mM $Ru(NH_3)_6^{3+}$ that does not form complexes with PAMAM G2-OH dendrimer. As shown in Fig. 8b, the reduction peak current of $Ru(NH_3)_6^{3+}$ shows a decrease with an increased amount of PAMAM G2-OH dendrimer due to the increase of viscosity of the solution. Correction of the titration results for Cd^{2+} - and Zn^{2+} -G2-OH complex formation by subtracting the current changes due to the viscosity changes yield an essentially flat current with $R > 4$ (Fig. 8c).

CVs for the Zn–PAMAM G2-OH dendrimer system are shown in Fig. 9. These are similar to the interaction of cadmium ions with dendrimers, with a negative potential shift and a peak current decrease after the complexation. The scan rate dependence and the CV for the mostly bound zinc ions show a diffusion control process (Fig. 9c). The greater negative potential shift for zinc ion reduction than that for cadmium ion in the presence of dendrimers can be explained by a stronger complexation of the dendrimers

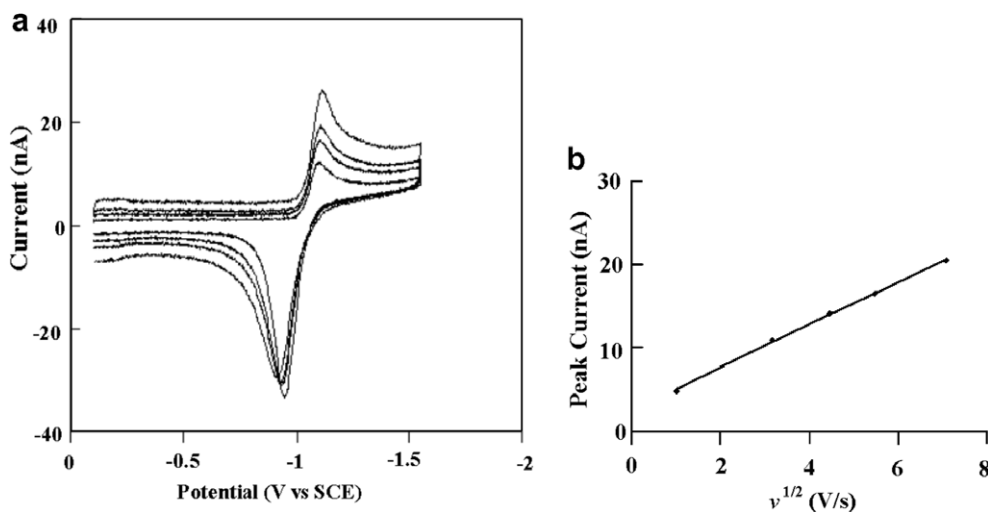


Fig. 6. Cyclic voltammograms of 0.6 mM $Zn(NO_3)_2$ (a) at increasing scan rate and the peak current dependence on the scan rate (b). Supporting electrolyte: 0.2 M $NaNO_3$. Electrode radius: 7 μm .

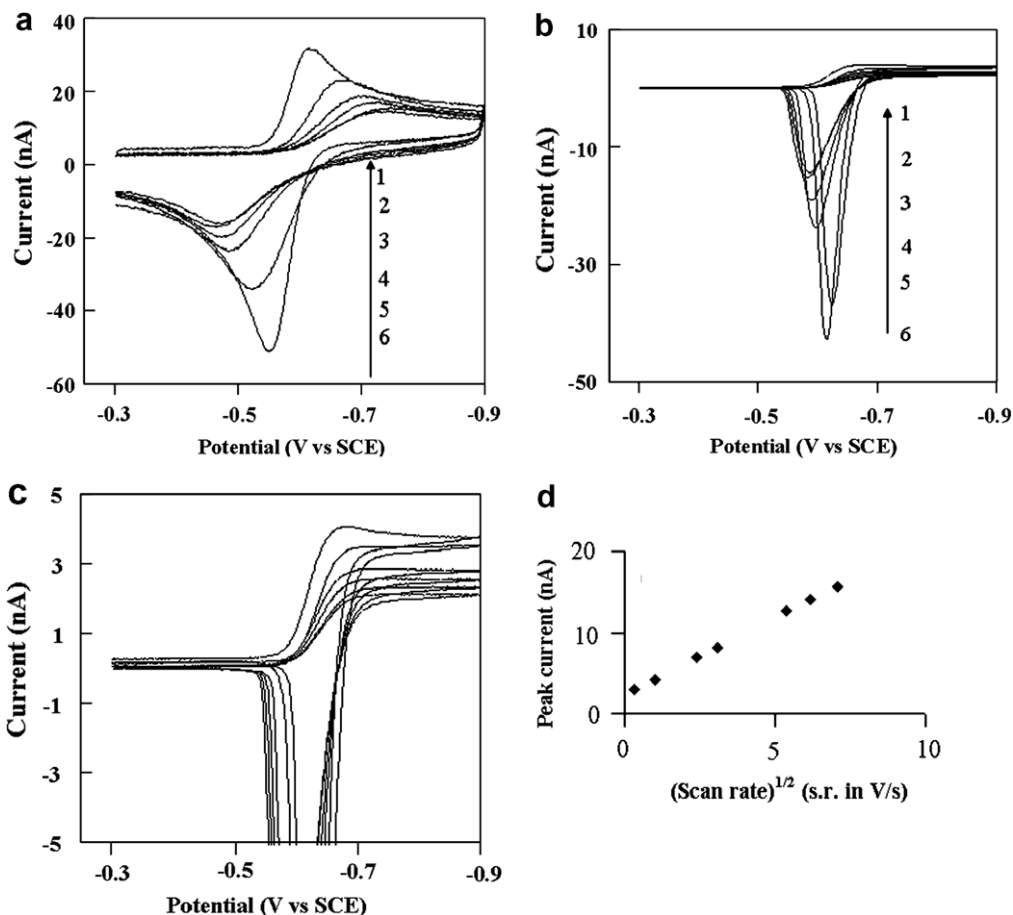


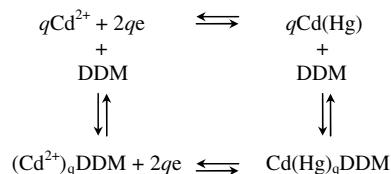
Fig. 7. Cyclic voltammograms of 0.6 mM Cd(NO₃)₂ upon the addition of various concentrations of dendrimer at a scan rate of 50 V/s (a); 0.05 V/s (b). The concentration of dendrimer are: 0 mM (1), 0.2 mM (2), 0.45 mM (3), 1 mM (4), 3 mM (5) and 6 mM (6), respectively; The arrows point to decreasing dendrimer concentration for decreasing anodic current. (c) is the expanded plot of b in the current range from -5 to 5 nA; (d) Scan rate dependence of the peak current of 0.6 mM Cd(NO₃)₂ with 1 mM dendrimer added. Supporting electrolyte: 0.2 M NaNO₃. Electrode radius: 7 μm.

with Zn²⁺. The decrease of the current is sharper compared with the cadmium complexes, which also suggests formation of complexes with a larger formation constant.

4. Theoretical model

Classically [25] the electrochemical (polarographic) study of complex ions was based on shifts in the half-wave potential with ligand concentration. Measurements based on the magnitude of the diffusion currents were ordinarily not made, because the diffusion coefficients and simple metal ion and complex were usually too similar to allow one to distinguish among the various complexes. However when a metal ion complexes with a large ligand, such as a polymer, one can also obtain valuable information about complexation by studying the change in limiting current with the ratio of metal ion and ligand. This approach has been used in investigations involving the intercalation of ruthenium complexes into DNA, for dendrimer–ferrocene-methanol electrostatic interactions, [26–30] and also in the dendrimer–silver ion complexation studies [13].

The theoretical approach assumes the following square scheme:



One assumes, based on the electrochemical behavior, that all electron transfer reactions are nernstian and that all complexation reactions involving bound and free species are at equilibrium:

$$E_{\text{b},q}^0 - E_{\text{f}}^0 = (0.059/2) \log(K_0/K_q) \quad (3)$$

where E_{f}^0 corresponds to the standard potential for the free metal ion electron transfer and $E_{\text{b},q}^0$ for the bound one, K_q is the equilibrium constant for the cumulative complexation of q metal ions and K_0 recognizes the possibility that the

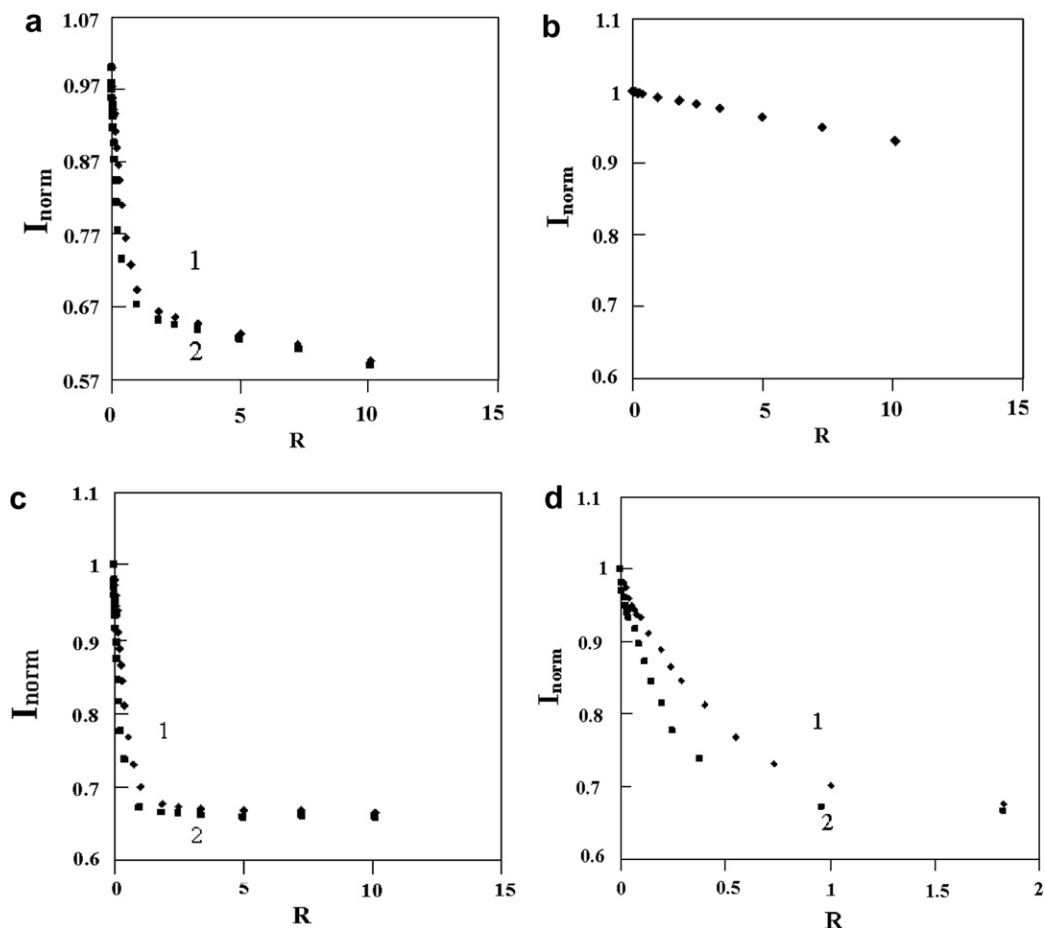


Fig. 8. Dependence of the normalized current on dendrimer concentrations for (a) 0.6 mM $\text{Cd}(\text{NO}_3)_2$ (1, \blacklozenge) and $\text{Zn}(\text{NO}_3)_2$ (2, \blacksquare) and (b) 0.6 mM $\text{Ru}(\text{NH}_3)_6^{3+}$. The data in (a) were corrected for the viscosity contribution using data from (b) and the corrected results are shown in (c). (d) is an expanded plot of (c) in the R range between 0 and 2.

zero valent metal remains associated with the dendrimer after reduction. The limiting potential shift for the cadmium–dendrimer interaction, at large R , was 0.080 V, which yields K_q/K_0 to be ~ 500 . Complexation of the zinc ions with the dendrimer at large R gives a potential shift of 0.136 V, which corresponds to the stability constant ratio K_q/K_0 to be $\sim 4 \times 10^4$. Such limiting stability constant ratios do not provide information about the individual complexation constants for smaller values of q . While this could be obtained in principle by studying the variation of the half-wave potential as a function of R , the rather small potential range would limit the precision of the reported values. Rather, we used the variation of the limiting current with R to construct a theoretical model to determine the stability constant K_q .

In the dendrimer titration experiments shown in Figs. 7–9 a solution of the free metal ion was prepared, dendrimer was added in small increments, and the limiting current as a function of R was determined. The first addition of a small amount of dendrimer ($R \ll 1$) leads to the formation of the polynuclear complexes containing the maximum number of metal ions per ligand. Further additions of dendrimer causes the dissociation of the complexes and forma-

tion of metal–dendrimer complexes with smaller q -values, finally dominated by $q = 1$ at the end of the titration. By assuming that all complexes formed have the same diffusion constant, D_b , the steady-state current can be expressed to be the sum of the reduction current of free and complexed diffusing species,

$$i = 2pnFD_r r[\text{Me}] + 2pnFD_b r \sum_{q=1}^q q[\text{Me}_q\text{L}] \quad (4)$$

where D_r is the diffusion coefficient of free metal ion and D_b the diffusion coefficient of the complexed metal. The measured diffusion coefficient of zinc complex is $3.6 \times 10^{-6} \text{ cm}^2/\text{s}$, which is smaller than that of cadmium–dendrimer complex, $4.6 \times 10^{-6} \text{ cm}^2/\text{s}$. The diffusion coefficient of the cadmium ions is also higher ($6.8 \times 10^{-6} \text{ cm}^2/\text{s}$) compared with zinc ions ($5.4 \times 10^{-6} \text{ cm}^2/\text{s}$) due to the smaller hydrated radius.

The steady-state current of Eq. (4) can be normalized using the current for totally free metal ions in the absence of dendrimer and

$$[\text{Me}_q\text{L}] = K_q[\text{Me}]^q[\text{L}] \quad (5a)$$

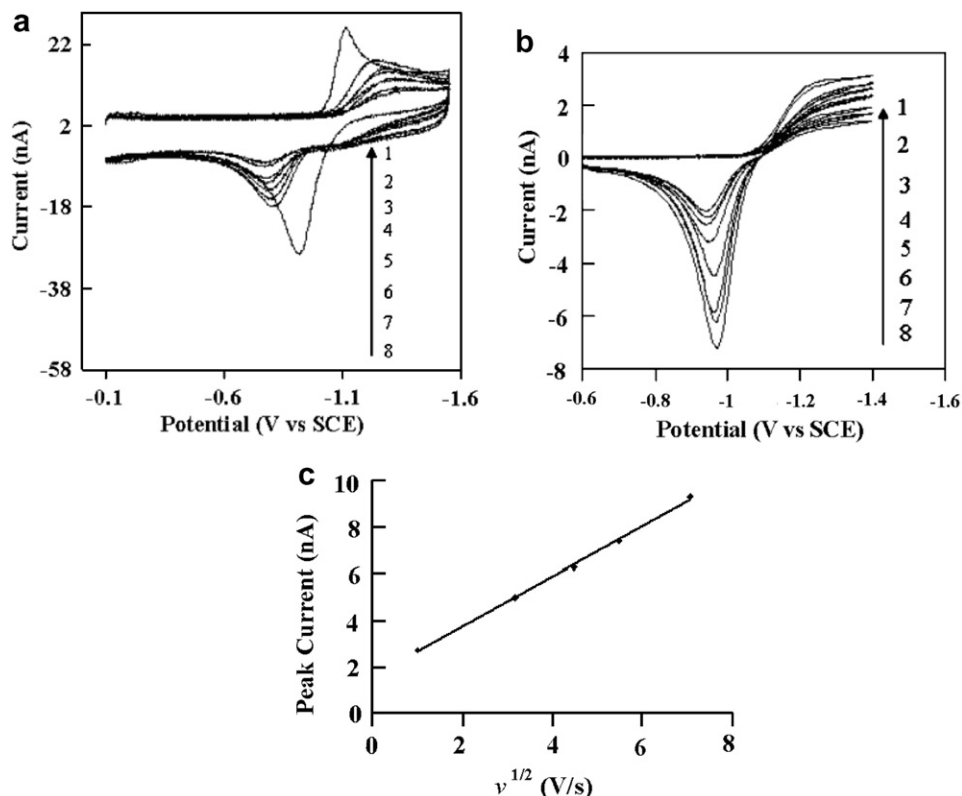


Fig. 9. Cyclic voltammograms of 0.6 mM Zn(NO₃)₂ upon the addition of various concentrations of dendrimer at a scan rate of 50 V/s (a); 0.05 V/s (b). The concentration of dendrimer are: 0 mM (1), 0.06 mM (2), 0.12 mM (3), 0.45 mM (4), 0.6 mM (5), 1 mM (6), 1.5 mM (7) and 4 mM (8), respectively; The arrows point to decreasing dendrimer concentration for decreasing anodic current. (c) Scan rate dependence of the peak current of 0.6 mM Zn(NO₃)₂ with 1 mM dendrimer added. Supporting electrolyte: 0.2 M NaNO₃. Electrode radius: 7 μm.

to obtain

$$i_{\text{norm}} = \frac{[\text{Me}]}{C_M} + \frac{D_b}{D_f C_M} \sum_{q=1}^q q K_q [\text{Me}]^q [\text{L}]$$

$$= \frac{[\text{Me}]}{C_M} + \frac{D_b}{D_f C_M} (C_M - [\text{Me}]) \quad (5b)$$

where C_M is the total metal ion concentration without addition of dendrimers. Free metal ion concentration $[\text{Me}]$ in the presence of dendrimer can therefore be derived from Eq. (5),

$$[\text{Me}] = \frac{\left(i_{\text{norm}} - \frac{D_b}{D_f}\right) C_M}{1 - \frac{D_b}{D_f}} \quad (6)$$

Using expressions (5) and (6) and the ones [31] related to the stability constant for each of the metal–dendrimer complex and its relation with free metal concentration $[\text{Me}]$ and free dendrimers $[\text{L}]$, we then get a direct relationship between the R and free metal concentration (see appendix). [32]

$$R = \frac{(C_M - [\text{Me}]) (\sum_{q=1}^q (K_q [\text{Me}] + 1))}{C_M \sum_{q=1}^q q K_q [\text{Me}]^q} \quad (7)$$

Since $[\text{Me}]$ is related to the normalized current (Eq. (6)) one can obtain the values of K_q from a plot of i_{norm} vs

R . The maximum value of q is obtained from consideration of the initial points of this plot, which in this case give a value of 4. The i_{norm} vs R curve was fit with a non-linear routine with four unknown equilibrium constants as adjustable parameters. The curves are shown in Fig. 10 and the equilibrium constants obtained are given in Table 1.

Note the different diffusion coefficients for the different metal ions for the 1:1 Me–dendrimer complex ($q = 1$). We are confident in these values since they are calculated from the steady-state current under conditions where no net changes in the current due to the complexation occur (i.e., no changes in $[\text{Me}]$ or D with $[\text{L}]$). This could indicate that the different metal–dendrimer complexes could also have different diffusion coefficients. It could be possible to add these parameters to the mathematical model, but at the expense of requiring many more experimental points to provide a statistically significant fit. However, our model, assuming all D are equal, fits the experimental results well. The difference in D for the Me–DEN complexes ($q = 1$), even though they follow the trend of the free ions, are within the same order of magnitude for the different metal ions and complexes ($3\text{--}7 \times 10^{-6} \text{ cm}^2/\text{s}$). However, the equilibrium constants vary 8 and 11 orders of magnitude for the Cd- and Zn-complexes. Thus, our results suggest that the changes of D

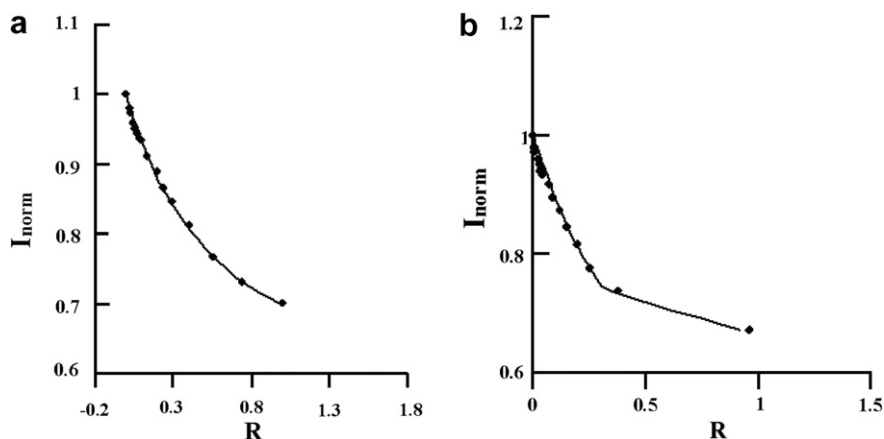


Fig. 10. Fit of the normalized peak current vs R . Plot concentration is 0.6 mM for both $\text{Cd}(\text{NO}_3)_2$ (a) or $\text{Zn}(\text{NO}_3)_2$ (b). Points are experimental values and line is fitted with the formation constants in Table 1.

Table 1

Four equilibrium constants for cadmium(II)–dendrimer and Zn(II)–dendrimer complexes determined by fitting the electrochemical titration results

	K_1 (M^{-1})	K_2 (M^{-2})	K_3 (M^{-3})	K_4 (M^{-4})
Cd^{2+}	1.3×10^5	1.6×10^9	3.3×10^{12}	4.6×10^{14}
Zn^{2+}	1.0×10^6	2.1×10^{11}	4.6×10^{14}	2.6×10^{17}

for the Me-DEN complexes or their effects are negligible and the equilibrium constants carry most of the weight on determining the voltammetric properties of these systems.

Consistent with our electrochemical study at a Hg UME, previous spectrophotometric titration studies of G2-OH dendrimer by copper (II) ions show a saturation number of the metals to be equal to 4. Cadmium, zinc and copper have similar complexation behavior with G2-OH dendrimer and a maximum stoichiometry of 4 can be obtained for all of these metal ions to form complexes with dendrimer. This is also can be seen as evidence that the interior amino groups are responsible for the complexation rather than the exterior hydroxyl groups. The fit of the experimental curve using four equilibrium constants was very close to the experimental data. Zinc ion forms stronger complexes compared to cadmium ion. These results are consistent with the earlier report on the complexes of zinc and cadmium with amines and ethylenediamines, [31] where the affinity of zinc ions to nitrogen groups has been shown to be higher than cadmium ions.

5. Conclusions

To conclude, reversible electrochemical behavior of cadmium and zinc ions can be obtained at the Hg UME. This electrode is easy to fabricate and it can be applied to the study of the coordination chemistry of dendrimers with metal ions. A square scheme can be used to explain the cadmium and zinc–dendrimer com-

plexation. The present study shows that cadmium and zinc can form stable complexes with dendrimer through its interior amino groups rather than exterior hydroxyl groups. In addition, zinc ion forms stronger complexes with dendrimer than cadmium ion. An electrochemical titration and measurement of the limiting current as a function of dendrimer:metal ratio was used to determine the stability constants of the metal–dendrimer complexes, with a maximum number of metal centers per dendrimer of 4. The procedure should also be applicable to larger dendrimers (e.g. generation 3...), but the greater number of complexed metal ions and smaller diffusion coefficient of D_b will complicate the treatment.

Acknowledgement

We gratefully acknowledge support of this research by the Robert A. Welch foundation.

Appendix A

The total metal concentration is equal to the sum of free metal concentration $[\text{Me}]$ and bonded ones with dendrimers,

$$C_M = [\text{Me}] + \sum_{q=1}^q q[\text{Me}_q\text{L}] \quad (\text{A.1})$$

where q is the number of metal ions coordinated to one dendrimer. The total dendrimer concentration C_D is composed of free dendrimers and the complexed ones

$$C_D = [\text{MeL}] + [\text{L}] \quad (\text{A.2})$$

with the stability constant for each metal–dendrimer complex,

$$K_q = \frac{[\text{Me}_q\text{L}]}{[\text{Me}]^q[\text{L}]} \quad (\text{A.3})$$

from which the concentration of each of the corresponding metal–dendrimer complexes can be derived,

$$[\text{Me}_q\text{L}] = K_q[\text{Me}]^q[\text{L}] \quad (\text{A.4})$$

using Eq. (A.4) to replace $[\text{Me}_q\text{L}]$ in Eq. (A.2), we obtain the expression for the total dendrimer concentration as function of free dendrimer $[\text{L}]$, free metal $[\text{Me}]$ and stability constants K_q ,

$$C_D = \sum_{q=1}^q K_q[\text{Me}]^q[\text{L}] + [\text{L}] \quad (\text{A.5})$$

therefore the free dendrimer concentration can be written as,

$$[\text{L}] = \frac{C_D}{\sum_{q=1}^q (K_q[\text{Me}]^q + 1)} \quad (\text{A.6})$$

Using Eqs. (A.1) and (A.3) to replace $[\text{L}]$ in the above equation by $[\text{Me}]$ and stability constants, we can obtain the following expression,

$$C_D = \frac{(C_M - [\text{Me}]) (\sum_{q=1}^q (K_q[\text{Me}] + 1))}{\sum_{q=1}^q q K_q [\text{Me}]^q} \quad (\text{A.7})$$

Rewriting the above equation by changing the position of C_D and C_M yields

$$C_M = [\text{Me}] + \frac{C_D \sum_{q=1}^q q K_q [\text{Me}]^q}{\sum_{q=1}^q (K_q [\text{Me}]^q + 1)} \quad (\text{A.8})$$

since $R = C_D/C_M$, Eq. (A.8) can be rewritten as Eq. (7) above.

References

- [1] D.A. Tomalia, H. Baker, J. Dewald, M. Hall, G. Kallos, S. Martin, J. Roeck, P. Smith, Polym. J. (Tokyo) 17 (1985) 117.
- [2] G.R. Newkome, F. Vögtle, Dendrimers and Dendrons, Wiley-VCH, Weinheim, 2002.
- [3] L. Balogh, D.R. Swanson, D.A. Tomalia, G.L. Hagnauer, A.T. McManus, Nano Lett. 1 (2001) 18.
- [4] H. Ye, R.M. Crooks, J. Am. Chem. Soc. 127 (2005) 4931.
- [5] H. Ye, R.M. Crooks, J. Am. Chem. Soc. 129 (2007) 3627.
- [6] Y. Xu, D. Zhao, Environ. Sci. Technol. 39 (2005) 2369.
- [7] Y. Xu, D. Zhao, Ind. Eng. Chem. Res. 45 (2006) 7380.
- [8] M.S. Diallo, S. Christie, P. Swaminatham, L. Balogh, X. Shi, W. Um, C. Papelis, W.A. Goddard, J.H. Johnson, Langmuir 20 (2004) 2640.
- [9] M.S. Diallo, S. Christie, P. Swaminatham, J.H. Johnson, W. Goddard, Environ. Sci. Technol. 39 (2005) 1366.
- [10] J. Garcia-Martinez, R.M. Crooks, J. Am. Chem. Soc. 126 (2004) 16170.
- [11] F.J.C. Rossotti, H. Rossotti, The Determination of Stability Constants and Other Equilibrium Constants in Solution, McGraw-Hill, New York, 1961.
- [12] D.C. Harris, Quantitative Chemical Analysis, seventh ed., Freeman and Company, New York, 2006.
- [13] F.-R.F. Fan, C.L. Mazzitelli, J.S. Brodbelt, A.J. Bard, Anal. Chem. 77 (2005) 4413.
- [14] K. Takada, D.J. Diaz, H.D. Abruña, I. Cuadrado, C. Casado, B. Alonso, M. Moran, J. Losada, J. Am. Chem. Soc. 119 (1997) 10763.
- [15] W. Ong, A.F. Kaifer, J. Am. Chem. Soc. 124 (2002) 9358.
- [16] Y. Bae, N. Myung, A.J. Bard, Nano Lett. 4 (2004) 1153.
- [17] J. Wang, Stripping Analysis: Principles Instrumentation and Applications, VCH Publishers, Deerfield Beach, FL, 1985.
- [18] K.R. Wehmeyer, R.M. Wightman, Anal. Chem. 57 (1985) 1989.
- [19] J. Mauzeroll, E. Hueske, A.J. Bard, Anal. Chem. 75 (2003) 3880.
- [20] A.J. Bard, L.R. Faulkner, Electrochemical Methods, Fundamentals and Applications, John Wiley & Sons, New York, 2001, p. 462.

- [21] W.T. De Vries, E.J. Van Dalen, Electroanal. Chem. 14 (1967) 315.
- [22] N. Donten, Z. Stojek, Z. Kublik, Electroanal. Chem. 163 (1984) 11.
- [23] M.A. Baldo, S. Daniele, G.A. Mazzocchin, Electrochim. Acta 41 (1996) 811.
- [24] (a) M.J. Rudolph, Electroanal. Chem. 543 (2003) 23;
(b) M.J. Rudolph, Electroanal. Chem. 571 (2004) 289;
(c) M.J. Rudolph, Electroanal. Chem. 558 (2003) 171;
(d) M.J. Rudolph, J. Comp. Chem. 26 (2005) 619;
(e) M.J. Rudolph, J. Comp. Chem. 26 (2005) 233;
(f) M.J. Rudolph, J. Comp. Chem. 26 (2005) 1193.
- [25] I.M. Kolthoff, J.J. Lingane, Polarography, second ed., Interscience, New York, 1952, p. 211.
- [26] T. Matsue, D.H. Evans, T. Osa, N.J. Kobayshi, J. Am. Chem. Soc. 107 (1985) 341.
- [27] M.T. Carter, A.J. Bard, J. Am. Chem. Soc. 109 (1987) 7528.
- [28] M.T. Carter, M. Rodriguez, A.J. Bard, J. Am. Chem. Soc. 111 (1989) 8901.
- [29] T.W. Welch, H.H. Thorp, J. Phys. Chem. 100 (1996) 13837.
- [30] A. Kulczynska, T. Frost, L.D. Margerum, Macromolecules 39 (2006) 7372.
- [31] L.G. Sillen, A.E. Martell, Stability Constants of Metal-ion Complexes, The Chemical Society, London, 1964.
- [32] The total metal concentration is equal to the summary of free metal concentration $[\text{Me}]$ and bonded ones with dendrimers

$$C_t = [\text{Me}] + \sum_{q=1}^q q[\text{Me}_q\text{L}] \quad (\text{A.1})$$

where q is the number of metal ions coordinated to one dendrimer. The total dendrimer concentration C_s is composed of free dendrimers and the complexed ones with metal ions,

$$C_s = [\text{MeL}] + [\text{L}] \quad (\text{A.2})$$

stability constant for each of the metal–dendrimer complex is,

$$K_q = \frac{[\text{Me}_q\text{L}]}{[\text{Me}]^q[\text{L}]} \quad (\text{A.3})$$

from which the concentration of each of the corresponding metal–dendrimer complexes can be derived,

$$[\text{Me}_q\text{L}] = K_q[\text{Me}]^q[\text{L}] \quad (\text{A.4})$$

using Eq. (A.4) to replace $[\text{Me}_q\text{L}]$ in Eq. (A.2), we got the expression for the total dendrimer concentration as function of free dendrimer $[\text{L}]$, free metal $[\text{Me}]$ and stability constants K_q ,

$$C_s = \sum_{q=1}^q K_q[\text{Me}]^q[\text{L}] + [\text{L}] \quad (\text{A.5})$$

therefore the free dendrimer concentration can be written as,

$$[\text{L}] = \frac{C_s}{\sum_{q=1}^q (K_q[\text{Me}]^q + 1)} \quad (\text{A.6})$$

using Eqs. (A.1) and (A.3) to replace $[\text{L}]$ in the above equation by $[\text{Me}]$ and stability constants, we can obtain the following expression,

$$C_s = \frac{(C_t - [\text{Me}]) (\sum_{q=1}^q (K_q[\text{Me}] + 1))}{\sum_{q=1}^q q K_q [\text{Me}]^q} \quad (\text{A.7})$$

Rewriting the above equation by changing the position of C_s and C_t yields

$$C_t = [\text{Me}] + \frac{C_s \sum_{q=1}^q q K_q [\text{Me}]^q}{\sum_{q=1}^q (K_q [\text{Me}]^q + 1)} \quad (\text{A.8})$$

since $R = \frac{C_s}{C_t}$, therefore Eq. (A.8) can be rewritten as

$$R = \frac{(C_t - [\text{Me}]) (\sum_{q=1}^q (K_q [\text{Me}] + 1))}{C_t \sum_{q=1}^q q K_q [\text{Me}]^q} \quad (\text{A.9})$$

which is Eq. (7) in the main text.